

# Consistent analysis of the elastic, inelastic and fusion cross sections in the systems $^{16}\text{O} + ^{144,148,150,152}\text{Sm}$ at sub-barrier energies

E. Guerra<sup>1</sup>, J. Lubian<sup>1</sup>, R. Cabezas<sup>2</sup>

**O**n the basis of the experimental data reported in the literature, an analysis of the elastic, inelastic and fusion cross sections was made for the  $^{16}\text{O} + ^{144,148,150,152}\text{Sm}$  systems at energies near the Coulomb barrier using a consistent deformed optical model potential. Coupled-channel calculations of the elastic and inelastic scattering cross sections were carried out using the ECIS87 code<sup>1</sup>.

In the present calculation the lowest  $0^+$ ,  $2^+$  and  $3^-$  states of the target nuclei  $^{144,148,150}\text{Sm}$  and the lowest  $0^+$ ,  $2^+$  and  $4^+$  states of  $^{152}\text{Sm}$  were included explicitly. The effects of Coulomb excitations were also taken into account.

The coupling potentials were generated following the usual deformed optical model potential prescription, using the harmonic vibrational model and the symmetric rotational model to describe the structure of the target nuclei.

By fitting procedure, a parameterization of the deformed optical potential was obtained that shows the so called "threshold anomaly". To calculate the fusion cross section by means of FRESKO code<sup>2</sup> this parameterization was used.

The calculated elastic and inelastic angular distributions and fusion excitation functions reasonably well agree with experimental data.

## I. Introduction

In recent years, nuclear reactions induced by heavy-ions have been widely investigated. In this kind of reactions, big amounts of energy and angular momentum are transferred between interacting nuclei. That is why many outgoing channels can be opened, such as: elastic and inelastic scattering, transfer reactions and fusion.

Specially, the reactions at energies near the Coulomb barrier have been the subject of great theoretical and experimental interest. In this region, some unexpected phenomena can occur, for example, the enhancement of fusion cross sections and "threshold anomalies" in the interacting potential. The term enhancement refers to the observed discrepancy between experimental measurements of fusion cross sections and theoretical predictions using one-dimensional models like Barrier Penetration Model<sup>3</sup> (BPM). This fact has been attributed to a lowering of the barrier due to the coupling to the transfer degrees of freedom<sup>4,5</sup>, static and dynamic deformations of the nuclei<sup>6-8</sup>, neck formation<sup>9</sup>, etc. Essentially, any process that provokes variations in barrier depth has the effect of varying the fusion cross sections. These variations favor the fusion process because, due to the non-linear behavior of the fusion cross section, one gain more in the fusion probability with the barrier lowering than one loose with its increasing.

<sup>1</sup> Center of Applied Studies for Nuclear Development, Havana, Cuba.

<sup>2</sup>Instituto de Física da Universidade Federal Fluminense, Niteroi, Brazil.

The anomaly consists in a rapid and localized energetic variation of the heavy-ion optical potential near the Coulomb barrier. Although some energy dependence can be expected through an energy variation in the effective nucleon-nucleon interaction, and from neglecting of non-locality in modeling the interaction with a local potential, the extent of the discrepancy at the lowest energies is much too large to be ascribed to these effects.

In previous works, the interaction of the  $^{16}\text{O}$  with the even-even samarium isotopes has been extensively studied<sup>10-13</sup>. Nevertheless, these studies have been carried out partially, that is, describing only some of the opened channels in these interactions. So, the aim of this paper is the simultaneous description of elastic, inelastic and fusion cross section of the systems  $^{16}\text{O} + ^{144,148,150,152}\text{Sm}$  by means of a unique optical potential. The influence of target deformation in fusion cross section is studied.

The organization of this paper is as follows. Section II will be devoted to analyze the elastic and inelastic scattering of  $^{16}\text{O}$  in the above mentioned targets. A parameterization of the deformed optical model potential is proposed in section III. In section IV the influence of target deformation in fusion cross section calculation is studied. Finally, we give our conclusions in section V.

## II. Elastic and inelastic scattering analysis

The study of elastic and inelastic heavy-ion scattering in even Samarium isotopes has vital interest to analyze the influence of target deformation in fusion cross section calculations near the Coulomb barrier.

The Samarium nuclei exhibit a wide range of deformations, from the spherical, semi-magic  $^{144}\text{Sm}$  to the well-deformed

$^{152}\text{Sm}$ . The use of a doubly magic projectile  $^{16}\text{O}$  was considered important to isolate effects that could be attributed to the target deformations.

As starting point to fit the optical potential parameters, the available data<sup>10,11</sup> of the differential elastic and inelastic cross sections for the systems  $^{16}\text{O} + ^{144}\text{Sm}$  at 66, 69.2 and 72.26 MeV,  $^{16}\text{O} + ^{148,150}\text{Sm}$  at 59, 62, 66 and 68 MeV and for  $^{16}\text{O} + ^{152}\text{Sm}$  at 59, 62, 66, 68 and 72 MeV were used.

The optical potential used has the form

where  $R_i = r_{oi} (A_t^{1/3} + A_p^{1/3})$  and  $a_i$  are the radii and diffusenesses of the real,

$$V(r) = U_o \cdot f(r, R, a) + i W_v f(r, R_v, a_v) + i W_s \cdot g(r, R_s, a_s) + V_{\text{coul}}(r).$$

imaginary volume and imaginary surface potential parts.  $A_t$  and  $A_p$  are the mass number of the target and the projectile respectively and  $r_{oi}$  are the reduced radii. The function  $f$  represents the Woods-Saxon form-factor and  $g$  its derivative. The last term stands for the Coulomb interaction between nuclei. The spin-orbit interaction was not considered because the spins of the interacting nuclei are zero.

The elastic and inelastic cross sections were calculated using the ECIS87 code, which solve the coupled-channel equation<sup>14</sup>. As structural model, the Harmonic Vibrator Model<sup>15</sup> (HVM), taking into account only one-phonon excitations, or Symmetric Rotational Model<sup>15</sup> (SRM) were considered depending on the excitation spectrum displayed by targets. In the case of the nuclei  $^{148,150}\text{Sm}$ , the parameters of optical potential were fitted using both models. A  $\chi^2$  iterative method<sup>1</sup> was used to fit optical potential parameters.

To select the coupled scheme the following criteria were considered:

- To take as coupled only the three lowest states of  $^{144}\text{Sm}$  (HVM),  $^{148}\text{Sm}$  (HVM),  $^{150}\text{Sm}$  (HVM) and  $^{152}\text{Sm}$  (SRM).

- To take as coupled only the two lowest states of  $^{148}\text{Sm}$  (SRM) and  $^{150}\text{Sm}$  (SRM).
- To consider only the ground state of  $^{16}\text{O}$  for all fits.

Some tests including the lowest  $2^+$  and  $3^-$  excited states of  $^{16}\text{O}$  were also run. Since the inclusion of these states was time consuming and the quality of fits changed less than 2%, they were not considered in the final calculations.

In Table 1 and Figure 1, the results of the fitted optical potential parameters and the theoretical calculated elastic cross sections for  $^{16}\text{O} + ^{144}\text{Sm}$  system are presented.

**Table 1.** Optical potential depths for  $^{16}\text{O} + ^{144}\text{Sm}$ . All values are in MeV.

Energy	$V_0$	$W_V$	$W_S$
66	105.0	2.5	1.21
69.2	130.0	43.0	5.4
72.26	115.0	88.0	3.18

The fitted geometrical parameters are:

$$\begin{aligned} r_o &= 1.2594 \text{ fm} & a_o &= a_v = 0.4 \text{ fm} \\ r_v &= 1.15 \text{ fm} & a_s &= 0.2 \text{ fm} \\ r_s &= 1.2623 \text{ fm} & r_c &= 1.2 \text{ fm} \end{aligned}$$

A successful description of differential elastic cross sections is achieved. Unfortunately, the data of inelastic cross sections are not available.

It can be seen from Figure 1 that the elastic cross section is overestimated for  $\theta > 100^\circ$ . It is well known, that nuclear interactions have great influence in cross sections for backward angles when the Coulomb interaction is present. That is why, another nuclear interaction, not considered in coupled scheme, could absorb part of the incident flux from elastic channel. In particular, appreciable cross section values of  $^{144}\text{Sm}(^{16}\text{O}, ^{14}\text{C})^{146}\text{Gd}$  and  $^{144}\text{Sm}(^{16}\text{O}, ^{12}\text{C})^{148}\text{Gd}$  transfer reactions are reported<sup>12,13</sup>. On the other hand, Landowne *et al.*<sup>16</sup> and Tenreiro *et al.*<sup>17</sup> have obtained similar overestimation in the backward angles for  $^{28}\text{Si}+^{58,64}\text{Ni}$ ,  $^{32}\text{S}+^{58,64}\text{Ni}$  and  $^{16}\text{O}+^{59}\text{Co}$  systems. Only with the inclusion of transfer channels in the coupled scheme, best results were achieved.

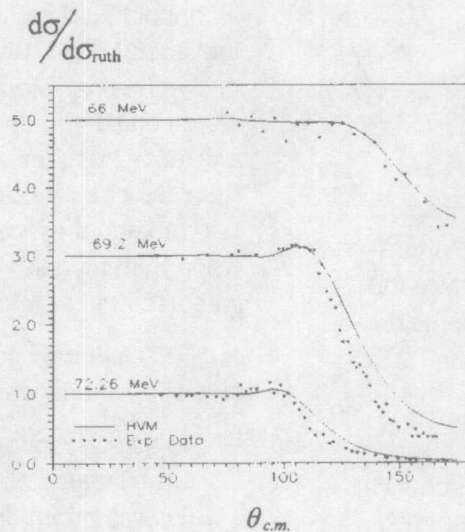
Figures 2-9 and Tables 2-3 show the obtained results for systems  $^{16}\text{O} + ^{148,150}\text{Sm}$ . The geometrical parameters for  $^{16}\text{O} + ^{148}\text{Sm}$  are:

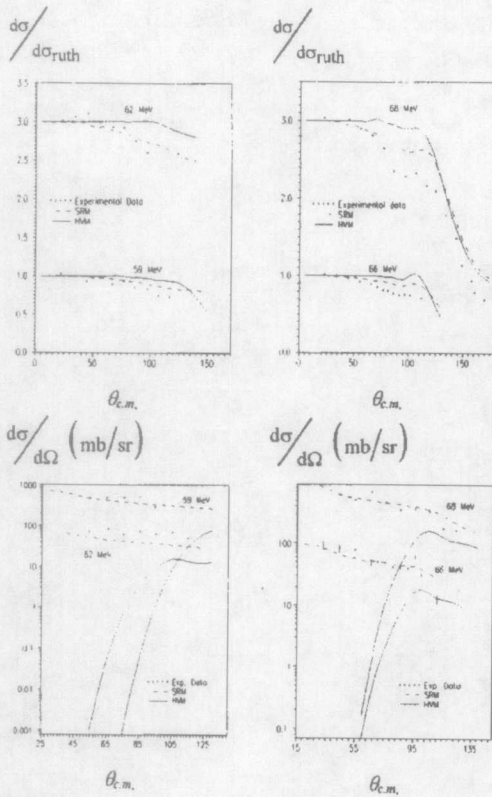
$$\begin{aligned} r_o &= 1.3 \text{ fm} & a_o &= 0.383 \text{ fm} \\ r_v &= 1.15 \text{ fm} & a_v &= 0.4 \text{ fm} \\ r_s &= 1.235 \text{ fm} & a_s &= 0.1 \text{ fm} \\ r_c &= 1.2096 \text{ fm} \end{aligned}$$

**Table 2.** Optical potential parameters for  $^{16}\text{O} + ^{148}\text{Sm}$ . All values are in MeV.

Energy	$V_0$	$W_V$	$W_S$
59	75.0466	3.0203	7.1601
62	84.0668	4.5204	5.6401
66	120.8289	5.0431	5.1088
68	95.0039	38.9288	20.0339

**Figure 1** Elastic scattering angular distribution for  $^{16}\text{O} + ^{144}\text{Sm}$ . The cross sections at  $E=59, 66$  MeV are multiplied by 3 and 5 respectively.





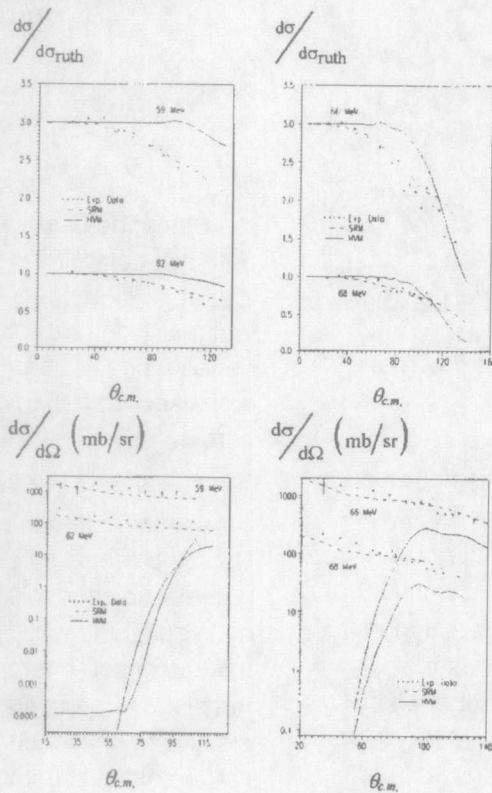
**Figures 2-5** Elastic and  $2^+$  state ( $E=0.55$  MeV) inelastic scattering angular distribution for  $^{16}\text{O} + ^{148}\text{Sm}$ . The elastic cross sections at  $E=59, 66$  MeV are multiplied by 3 and the inelastic ones are multiplied by 10.

The geometrical parameters for  $^{16}\text{O} + ^{150}\text{Sm}$  are the following:

$$\begin{aligned} r_o &= 1.2629 \text{ fm} & a_o &= 0.4 \text{ fm} \\ r_v &= 1.25 \text{ fm} & a_v &= 0.4 \text{ fm} \\ r_s &= 1.2667 \text{ fm} & a_s &= 0.2 \text{ fm} \\ r_c &= 1.2473 \text{ fm} \end{aligned}$$

**Table 3.** Optical potential depths for  $^{16}\text{O} + ^{150}\text{Sm}$ . All values are in MeV.

Energy	$V_o$	$W_v$	$W_s$
59	85.0	4.0	40.52
62	90.0245	22.68	21.82
66	107.3246	40.68	3.823
68	117.1242	30.111	30.5204



**Figures 6-9.** Elastic and  $2^+$  state ( $E=0.3334$  MeV) inelastic scattering angular distribution for  $^{16}\text{O} + ^{150}\text{Sm}$ . The elastic cross sections at  $E=59, 66$  MeV are multiplied by 3 and inelastic ones are multiplied by 10.

From figures 2-9, it can be seen that the SRM achieves better results for both systems because Coulomb corrections for the forward angles are significant while for the HVM they are negligible. Even though, both targets have low-lying states which nature can not be described by the SRM. The use of a more realistic model, like the Davydov-Chaban Model<sup>18</sup>, could report better results.

The elastic cross section is overestimated too at some energies for backward angles. The physical reason of this overestimation was explained above and the probably way of improving these calculations is the same. In the literature<sup>12,13</sup> appreciable transfer cross sections for these nuclei are reported too.

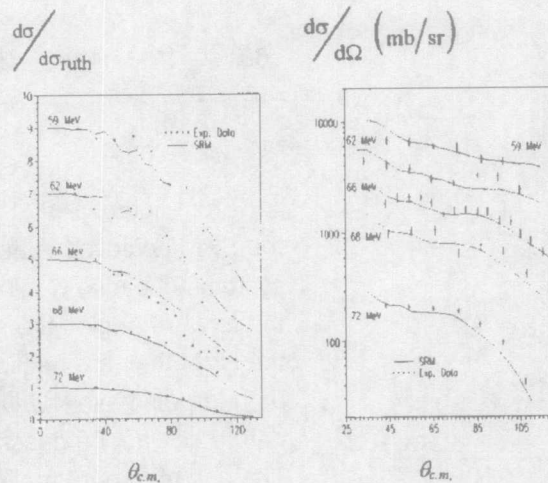
To describe the low-lying states of  $^{152}\text{Sm}$ , the SRM was used including quadrupole and hexadecapole modes.

It is important to emphasize that it was necessary to fit the quadrupole deformation parameter  $\beta_2$  because the available data are ambiguous. The obtained value ( $\beta_2 = 0.2224$ ) is quite similar to the one obtained by P.R.S.Gomes<sup>7</sup> in a recent work.

The fits of geometrical parameters for the  $^{16}\text{O} + ^{152}\text{Sm}$  system reported the following results:

$$\begin{aligned} r_o &= 1.2727 \text{ fm} & a_o &= 0.4 \text{ fm} \\ r_v &= 1.193 \text{ fm} & a_v &= 0.4 \text{ fm} \\ r_s &= 1.5 \text{ fm} & a_s &= 0.1 \text{ fm} \\ r_c &= 1.3 \text{ fm} \end{aligned}$$

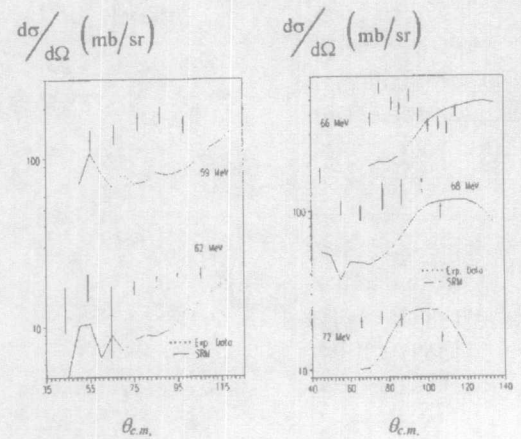
**Figures 10-11**  
Elastic and  $2^+$  state ( $E = 0.1218 \text{ MeV}$ ) inelastic scattering angular distribution for  $^{16}\text{O} + ^{152}\text{Sm}$ . The elastic cross sections at  $E=68, 66, 62$  and  $59 \text{ MeV}$  are multiplied by 3, 5, 7 and 9 respectively. The inelastic ones are multiplied by 5, 10, 20 and 40.



Even though the SR Model is not a bad approximation, the description of the  $4^+$  state inelastic cross section is not good. This fact could be provoked by asymmetric effects not taken into account by this model. The use of more realistic model as the Asymmetric Rotational Model proposed by A.Davydov and G.F.Filippov<sup>19</sup> could improve the results.

**Table 4.** Results of optical potential parameters for  $^{16}\text{O} + ^{152}\text{Sm}$ . All values are in MeV.

Energy	$V_o$	$W_v$	$W_s$
59	77.3	16.1905	28.7
62	78.9	32.2105	12.2062
66	84.0	36.19	7.706
68	86.7	40.59	6.5
72	81.8	50.0	7.2562



**Figures 12-13.**  $4^+$  state ( $E = 0.3665 \text{ MeV}$ ) inelastic scattering angular distribution for  $^{16}\text{O} + ^{152}\text{Sm}$ . The inelastic cross sections are multiplied by 5, 10 and 20 for  $E = 68, 59,$  and  $66 \text{ MeV}$  respectively.

### III. Parameterization

Using the best values of the optical potential parameters obtained from fits, an energetic dependence of the real and imaginary depths was found. This dependence will permit to calculate the cross sections at any energy near Coulomb barrier.

The conduct of the absorptive potential is easy to understand qualitatively. The Coulomb repulsion effectively closes the non-elastic channels at sub-barrier energies by keeping the colliding ions apart. Increasing the energy allows non-elastic reactions to proceed and absorption from elastic channel occurs. The behavior of the real potential is unexpected even though it

is understood to be a necessary accompaniment to the variation of absorption.

Taking into account these criteria, a schematic model has been proposed<sup>20</sup> for the imaginary potential behavior  $W(E) = W_V + W_S$ . It has the advantage of giving a simple analytic form for the dispersion relations proposed by Mahaux *et al.*<sup>21</sup>. Although this schematic behavior has the unphysical feature of discontinuities in the slope of  $W(E)$ , it gives results remarkably close to more physical, smooth functions for  $W(E)$ .

In this model,  $W(E)$  is represented by a series of linear segments. The used expression was the following:

$$W(E) = W_I + \Delta W(E),$$

where

$$\Delta W \begin{cases} 0 & \text{for } E \leq E_a \\ W_0 \left( \frac{E - E_a}{E_b - E_a} \right) & \text{for } E_b > E > E_a \\ W_0 & \text{for } E \geq E_b \end{cases}$$

and the parameters  $W_0$ ,  $E_a$  and  $E_b$  are varied to adjust the real potential.

Using the last equation and the dispersion relations, the following expression was obtained for real potential:

$$V_0(E) = V_I + \Delta V(E),$$

with

$$\Delta V(E) = \frac{W_0}{\pi} (\epsilon_a \ln|\epsilon_a| - \epsilon_b \ln|\epsilon_b|)$$

where

$$\epsilon_i = \frac{E - E_i}{E_b - E_a}$$

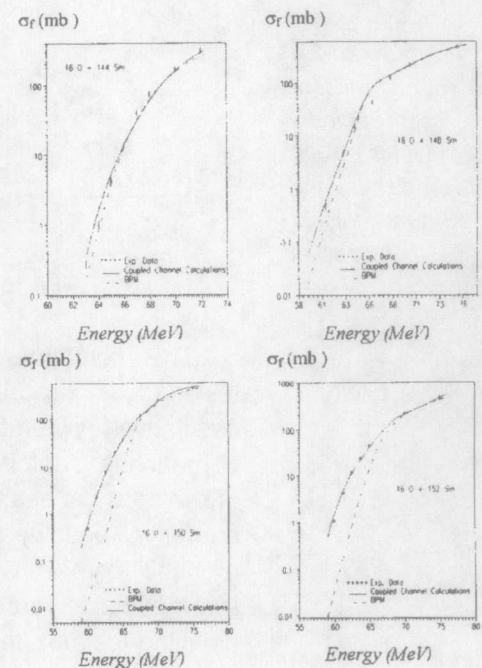
Figures 18-21 show the behavior of real and imaginary potential depths using the above expressions for real and imaginary potential depths. Rapid variations of real and imaginary potential depths near the

fusion threshold are observed. These variations are the so called "threshold anomalies". The application of these dispersion relations to recent phenomenological analyses has been remarkably successful<sup>22,23</sup>.

#### IV. Fusion analysis

The observed enhancement in fusion cross section in heavy-ion interactions has stimulated many theoretical studies. Some of the possible causes of discrepancy between experimental measurements and one-dimensional models were mentioned above. In the present paper only the influence of target deformation was considered.

For fusion cross section calculations the coupled-channel formalism and the Barrier Penetration Model implemented in the FRESKO code were used. To perform the calculations, the obtained parameterization was used. In figures 14-17, the results of these calculations are shown.



Figures 14-17. Fusion cross sections for  $^{16}\text{O} + ^{144,148,150,152}\text{Sm}$  systems. Experimental data taken from ref. 6 for  $^{144}\text{Sm}$  and ref. 24 for the others.

It can be seen that the BPM fails in the description of fusion cross sections below the Coulomb barrier. The discrepancy grows with the energy decrease because at low energies, the structure effects are more important.

During the fits of geometrical optical parameters an interesting singularity was observed: the diffuseness of the surface imaginary potential ( $a_s$ ) was reduced considerably to fit the fusion cross sections. This fact can suggest that the processes that enhance fusion cross section are localized in the region where nuclei are "grazing". It would be interesting to study if the transfer reaction potentials obey this behavior. This work is in progress.

## V. Conclusions

All the different processes involved in any nuclear reaction are submitted to the physical idea of a unique interaction potential between two colliding nuclei. In the present paper, following this idea a reasonable well description of the main processes in  $^{16}\text{O} + ^{144,148,150,152}\text{Sm}$  reactions was achieved.

In the description of  $^{16}\text{O} + ^{148,150}\text{Sm}$  systems a comparison between HVM and SRM was carried out. Although the SRM achieves better results than HVM, this model is a drastic approximation to the nuclear structure of both targets. The use of more realistic models could report better results.

The inclusion in coupled channel calculations of Coulomb Corrections was the key to fit inelastic cross sections angular distributions in the SRM.

The enhancement of fusion cross section was explained by the inclusion of the target deformations in the coupled channel formalism. The BPM calculation fails for energies below the Coulomb barrier. The magnitude of the failure increases with growing deformations.

The "threshold anomalies" of the potential were observed. An energy dependence of optical potential was found using a certain useful dispersion relation.

**Figure 18-19.**  
Energy-dependent optical model potential for  $^{144}\text{Sm}$  (dashed lines) and  $^{150}\text{Sm}$  (solid lines) nuclei.

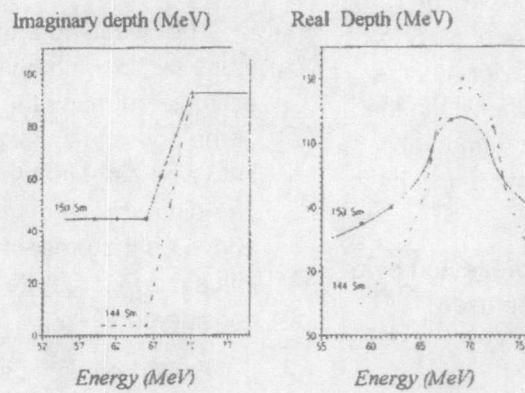
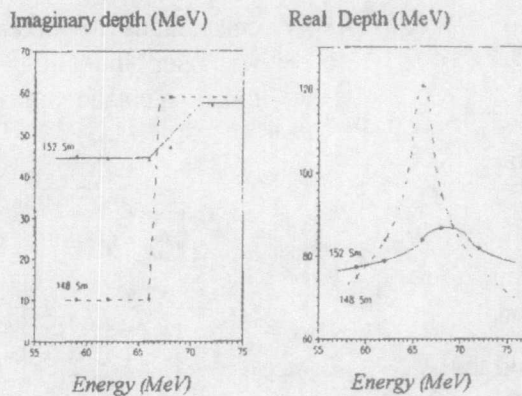


**Figure 20-21.**  
Energy-dependent optical model potential for  $^{148}\text{Sm}$  (dashed lines) and  $^{152}\text{Sm}$  (solid lines) nuclei.



The effect of target deformation on the fusion cross section can be understood qualitatively. When the spherical projectile approaches a deformed nucleus with axis of symmetry at beam direction (prolate), the barrier will be lowered and the fusion probability grows. When the target has its symmetry axis perpendicular to the beam direction (oblate), the barrier will be increased and the fusion probability will be reduced. When the nuclear shape is almost spherical, it can be stated that the greater fluctuations of the nuclear shape the bigger fusion cross section.

## References

1. J.Raynal, Procc. of the Workshop on Applied Nuclear Theory and Nuclear Model Calculations for Nuclear Technology Applications, *Trieste, Edited by M.K.Mehta and J.J.Schmidt, World Scientific Singapore 1989 pag. 506.*
2. I.J.Thompson, *Comp. Phys. Rep.* **7** (1988) 167.
3. C.Y.Wong, *Phys. Rev. Lett.* **31** (1973) 766.
4. R.A.Brogliola *et al.*, *Phys. Rev.* **C27** (1983) 243.
5. K.Zhao *et al.*, *Nucl. Phys.* **A586** (1995) 483.
6. D.Digregorio *et al.*, *Phys. Lett.* **B176** (1986) 322.
7. P.R.S.Gomes, Procc. of JAERI International Symposium on Heavy-Ion Reactions Dynamics in Tandem Energy Region, *Hitachi Japan (1988) pag.21.*
8. R.Vandenbosh, *Annu. Rev. Nucl. Part. Sci.* **42** (1992) 447.
9. A.Iwamoto and K.Harada, *Z. Phys.* **A326** (1987) 201.
10. D.Aabriola *et al.*, *Phys. Rev.* **C39** (1989) 546.
11. P.Talon *et al.*, *Nucl. Phys.* **A359** (1981) 493.
12. G.Marchesseau, " Etude des Reactions de Transfert ( $^{16}\text{O}, ^{12}\text{C}$ ) et ( $^{16}\text{O}, ^{14}\text{C}$ ) sur les Isotopes Pairs-Pairs de Samarium au Voisinage de la Barrière Coulombienne" Tese do Doutorado pela Universidade de Paris-Sud, Centre D'Orsay, *Paris, France, (1978).*
13. A.M.M.Maciél, " Reações de Transferencia em  $^{16}\text{O} + \text{ASm}$  ", Disertação realizada como requisito para a obtenção do título de Mestre em Física, *UFF, Niteroi, Brasil, 1993.*
14. T.Tamura, *Rev. Mod. Phys.*, **37** (1965) 679.
15. J.M.Eisemberg y W.Greiner, "Nuclear Models. Collective and Single Particle Phenomena", Noth-Holland Publ.Co., *Amsterdam (1970).*
16. S.Landowne, Workshop on Heavy Ion Collisions at Energies Near the Coulomb Barrier, *July 5-7, England, (1990).*
17. C.Tenreiro *et al.*, *Phys. Rev.* **C49** (1994).
18. A.S.Davydov and A.A.Chaban, *Nucl. Phys.* **20** (1960) 499.
19. A.S.Davydov y G.F.Filippov, *Zh. E.T.F.* **35** (1958) 440.
20. R. Lipperheide and A.Schmidt, *Nucl. Phys.* **A372** (1968) 65.
21. C.Mahaux, H. Ngo and G.R.Satchler, *Nucl. Phys.* **A449** (1986) 354.
22. C.H.Johnson, D.J.Horen and C.Mahaux, *Phys. Rev.*, **C36** (1987) 2252.
23. C.Mahaux and R.Sartor, *Nucl. Phys.* **A493** (1989) 157.
24. R.G.Stokstad *et al.*, *Phys. Rev.*, **C21** (1981) 2427. *Phys. Rev. Lett.*, **41** (1978) 465.